Boron-Doped P+ Nanocrystalline Diamond Gate Electrode for AlGaN/GaN HEMTs

Andrew D. Koehler, Travis J. Anderson, Karl D. Hobart, Marko J. Tadjer, Tatyana I. Feygelson, Jennifer K. Hite, Bradford B. Pate, Francis J. Kub, and Charles R. Eddy, Jr.

Naval Research Laboratory, Washington DC 20375, andrew.koehler@nrl.navy.mil, 202-404-6788

Keywords: GaN, HEMT, Diamond, Heat Spreading, Thermal Management

Abstract

Boron-doped p+ nanocrystalline diamond (B-NCD) gate electrodes were integrated on AlGaN/GaN high electron mobility transistors (HEMTs) to provide improved thermal management during high power operation. B-NCD gated HEMTs demonstrate improved maximum drain current, lower on-resistance, and reduced gate leakage current compared to conventional reference HEMTs fabricated on samples from the same AlGaN/GaN-on-Si wafers. Since NCD is a high thermal conductivity material, implementing the B-NCD as a gate electrode places the heat-spreading layer in direct contact with the source of self-heating, at the drain side of the gate. Also, the B-NCD gate electrodes are thermally and chemically stable, allowing for integration with thicker topside NCD heat spreading layers for advanced thermal management.

INTRODUCTION

AlGaN/GaN high electron mobility transistors (HEMTs) are an appealing technology for high power, high frequency, and high voltage power switching applications, however self-heating during operation limits their performance. Thermal management provided by diamond heat spreading layers has been investigated as a method to mitigate device self-heating, however backside approaches are limited by sample size, thickness, availability, and coefficient of thermal expansion (CTE) mismatch. Also, topside nanocrystalline diamond (NCD) heat spreading films have been demonstrated to provide a scalable process, capable of placing the heat spreading film adjacent to the heat source, at the drain edge of the gate, without degrading the electrical performance of the device [1-3]. NCD thin films offer extremely high thermal conductivity, small grain size, and optical transparency [4].

Here, an supplementary step is taken toward dissipating the heat away from the device active area. A p+ B-doped NCD (B-NCD) gate electrode has been integrated with the AlGaN/GaN HEMT [5]. The B-NCD gated device offers advantages for power switching devices and applications since the B-NCD gate electrode is directly located at the heat source during high power operation. This high thermal conductivity gate material assists in heat spreading, and can be combined with topside NCD heat spreading films due to the thermal and chemical stability of the gate contact. Also, since NCD is optically transparent, top down optical characterization can be performed on B-NCD gated HEMTs.

EXPERIMENT

Reference Ni/Au Schottky-gated and novel B-doped p+ NCD-gated GaN HEMTs were fabricated on pieces of the same GaN-on-Si wafer with an 18 nm $AlGa_{0.27}Ga_{0.73}N$ barrier. Each sample was processed identically until the gate electrode deposition step. First, a Cl_2-based inductively coupled plasma (ICP) etch was used form the mesa isolation. Then, Ti/Al/Ni/Au Ohmic contacts were deposited by e-beam evaporation and patterned by lift-off. The devices were then passivated with 50 nm of SiN_x by plasma-enhanced chemical vapor deposition (PECVD). Recess openings were etched in the PECVD SiN_x passivation layers by an SF_6-based reactive ion etch (RIE). The reference samples were then patterned with e-beam evaporated Ni/Au gates followed by lift-off, while the B-NCD HEMTs received 500 nm of p+ boron doped NCD. The sheet resistance and doping density of the B-NCD films were R_{SH} = 400 Ω/□, N_A = 7.5x10^{19} cm^{-3}, respectively. The B-NCD created a conformal layer over the entire sample, using seeding and growth methods reported in the literature [6,7].

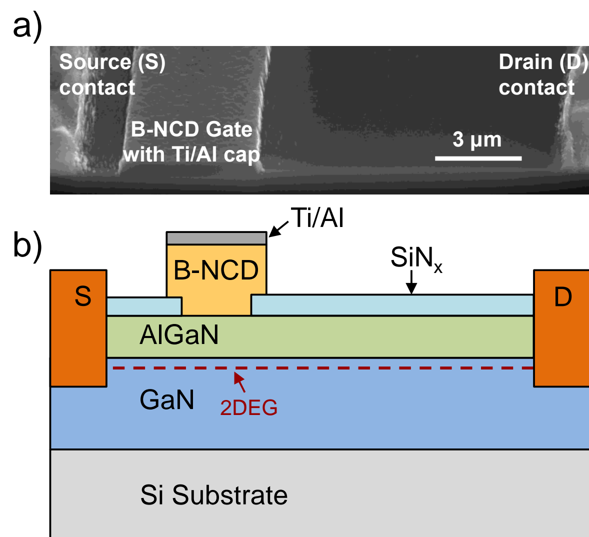

Figure 1. Cross-section of B-NCD gated AlGaN/GaN HEMT shown by a) focused ion beam (FIB) cross-section and a b) schematic cross section.

6

The gate electrode features were patterned by an O_2-based ICP etch, using Al as a hard mask and the SiN_x passivation as an etch stop. The Al mask was left in place to serve as self-aligned Ohmic contacts to the B-NCD gate. A focused ion beam (FIB) cross-section and schematic cross-section of the B-NCD gated HEMT is shown in Figure 1.

The reference and B-NCD-gated samples were characterized by DC *I-V* and Hall measurements. The DC *I-V* curves were taken on HEMTs with single gate fingers (100-µm wide), with a gate-to-source spacing of 2 µm, gate-to-drain spacing of 15 µm, and gate lengths of 5 µm. Whereas, the Hall measurements were taken on 100 μm^2 gated van der Pauw structures on the same die as the HEMTs.

RESULTS AND DISCUSSION

The first growth of B-NCD gate electrode films yielded devices with a large negative threshold voltage (V_T = -19.50 V), compared to the Ni/Au reference HEMTs (V_T = -2.13 V). This large shift is attributed to the presence of a thin insulating or lightly doped NCD layer at the semiconductor-NCD interface, caused by lag in the boron flow during initial NCD growth. The wide bandgap NCD acts as a gate dielectric, shifting the V_T. Figure 2 shows the measured *I-V* curves comparing the reference device to the B-NCD Gate Growth #1 with a large shift in V_T.

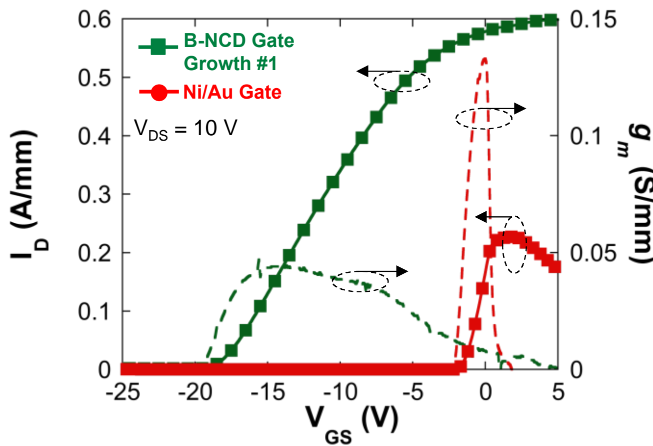

Figure 2. Drain current versus gate voltage characteristics for the first growth of B-NCD as a gate electrode for AlGaN/GaN HEMT, showing a large negative V_T shift compared to the Ni/Au reference HEMT.

To enhance the boron doping level of the NCD near the semiconductor-NCD interface, a second growth was performed where the boron flow was initiated prior to NCD growth. As shown in Figure 3, HEMTs with B-NCD Gate Growth #2, and increased boron doping density, resulted in a significantly improved threshold voltage (V_T = -2.91 V). Also, the B-NCD gated HEMTs demonstrated improvement in the maximum drain current ($I_{D,max}$).

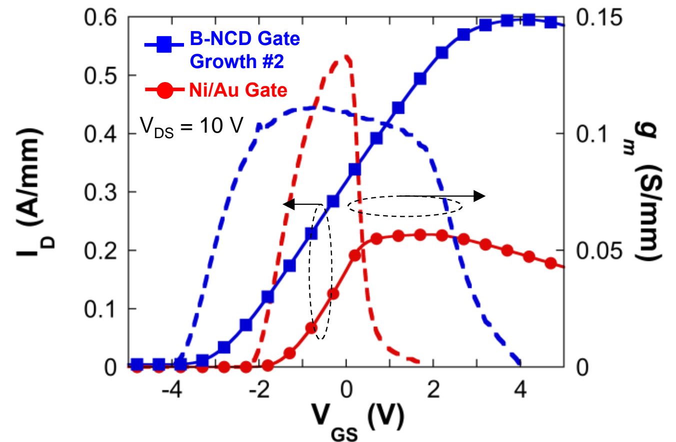

Figure 3. Drain current versus gate voltage characteristics for the second growth of B-NCD as a gate electrode for AlGaN/GaN HEMT, showing a reduced negative V_T shift compared to the Ni/Au gated reference HEMT.

A comparison between the Hall and *I-V* characteristics for both B-NCD gated HEMTs and the reference Ni/Au gated HEMTs is shown in Table 1. The B-NCD gated HEMTs show improvements in the two-dimensional electron gas mobility (μ_{2DEG}), sheet carrier density (n_s), and sheet resistance (R_{SH}). Likely, the cause for these improvements are related to additional tensile strain induced on the AlGaN barrier from the NCD.

The Hall characteristics between the B-NCD Gate Growth #1 and B-NCD Gate Growth #2 are nearly identical indicating that the saturation of the growth chamber before NCD growth had little to no impact on the 2DEG properties. However, the improvements in boron doping near the NCD-semiconductor interface in the second growth resulted in improved gate control of the 2DEG channel and improved device operation. Figure 4 shows Drain current versus drain voltage characteristics for the second B-NCD gated HEMT. The reduction in on-resistance and increase in maximum drain current is shown compared to the reference Ni/Au gated HEMT.

TABLE I
DEVICE PARAMETERS FOR SCHOTTKY AND NCD-GATED HEMT CONFIGURATIONS FOR BOTH FIRST AND SECOND DIAMOND GROWTHS.

Parameter	Units	Ni/Au Gate	NCD Gate #1	NCD Gate #2
μ_{2DEG}	cm²/(V·s)	1220	1280	1280
n_s	cm^{-2}	$8.92x10^{12}$	$1.02x10^{13}$	$1.02x10^{13}$
R_{SH}	Ω/□	533	478	478
R_{ON}	Ω-mm	29.4	10.1	12.1
I_{DS} (V_G = 0V)	A/mm	0.198	1.07	0.217
I_{OFF} (V_G = -10V)	A/mm	$8.04x10^{-5}$	$9.12x10^{-3}$	$9.12x10^{-6}$
V_T	V	-2.13	-19.5	-2.91

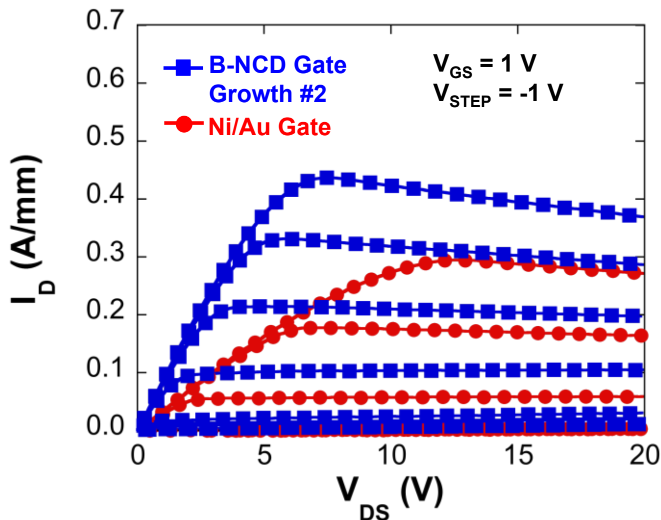

Figure 4. Drain current versus drain voltage characteristics for the second B-NCD gated HEMT. The reduction in on-resistance and increase in maximum drain current is shown compared to the reference Ni/Au gated HEMT.

As shown in Figure 5, the gate leakage current in the forward and reverse bias conditions is reduced. This is advantageous during normal operation, but also allows for the HEMT to be driven farther in the forward bias region to provide higher drain current. Increased boron doping levels near the semiconductor-NCD interface will likely deplete the 2DEG under the gate. Combined with the ability to forward bias the gate, these attributes could enable normally off operation. Also, the optically transparent B-NCD gate will enable top-down optical characterization through the gate, such as electroluminescence and micro-Raman spectroscopy.

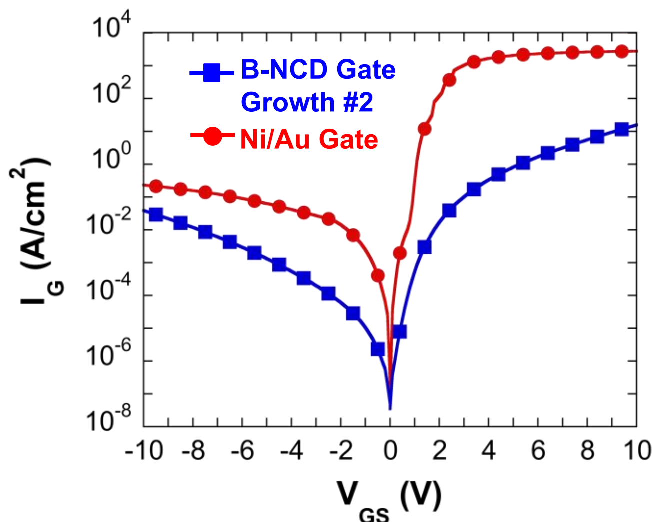

Figure 5. Gate current versus gate voltage characteristics shown with the source and drain terminals grounded. Reduction in gate current is observed for the second B-NCD gated HEMT.

Conclusions

In conclusion, novel boron-doped nanocrystalline diamond (B-NCD) gated AlGaN/GaN HEMTs have been demonstrated to offer superior performance over reference Ni/Au gated HEMTs. B-NCD gate electrode place high thermal conductivity material in direct contact with the heat source of the HEMT during high power operation, offering improved thermal management.

Acknowledgements

Work at the U.S. Naval Research Laboratory is supported by the Office of Naval Research. The authors are grateful to the NRL Nanoscience Institute staff. M.J.T. acknowledges support of the ASEE-NRL postdoctoral fellowship program.

6

References

[1] M.J. Tadjer, T.J. Anderson, K.D. Hobart, T.I. Feygelson, J.D. Caldwell, C.R. Eddy, Jr, F.J. Kub, J.E. Butler, B.B. Pate, J. Melngailis. "Reduced self-heating in AlGaN/GaN HEMTs using nanocrystalline diamond heat-spreading films" *IEEE Electr. Dev. Lett*. Vol. 33, no. 1 (2012) pp. 23-25.

[2] T.J. Anderson, A.D. Koehler, M.J. Tadjer, K.D. Hobart, T.I. Feygelson, B.B. Pate, F.J. Kub, "Process Improvements for an Improved Diamond-capped GaN HEMT Device" *CS MANTECH Conference*, May 13th - 16th, 2013, New Orleans, Louisiana, pp. 206-208.

[3] T.J. Anderson, K.D. Hobart, M.J. Tadjer, A.D. Koehler, T.I. Feygelson, J.K. Hite, B.B. Pate, F.J. Kub, C.R. Eddy, "Nanocrystalline Diamond for near Junction Heat Spreading in GaN Power HEMTs" *Compound Semiconductor Integrated Circuit Symposium*, 2013 IEEE 13-16 Oct. 2013 pp. 1-4.

[4] J.E. Butler and A.V. Sumant, "The CVD of nanodiamond materials," *Chem. Vapor Deposition*, vol. 14, nos. 7–8 pp. 145–160, 2008.

[5] T.J. Anderson, A.D. Koehler, K.D. Hobart, M.J. Tadjer, T.I. Feygelson, J.K. Hite, B.B. Pate, F.J. Kub, and C.R. Eddy, Jr, "Nanocrystalline Diamond-Gated AlGaN/GaN HEMT" *IEEE Electr. Dev. Lett*. Vol. 34, No. 11 (2013) pp. 1382-1384.

[6] K.D. Chabak, J.K. Gillespie, V. Miller, A. Crespo, J. Roussos, M. Trejo, D.E. Walker, Jr., G.D. Via, G.H. Jessen, J. Wasserbauer, F. Faili, D.I. Babić, D. Francis, and F. Ejeckam, "Full-wafer characterization of AlGaN/GaN HEMTs on free-standing CVD diamond substrates" *IEEE Electr. Dev. Lett.*, vol. 31, no. 2, (2010) pp. 99.

[7] J.E. Butler and A.V. Sumant, "The CVD of nanodiamond materials" *Chemical Vapor Deposition*, 14, 145 (2008).

Acronyms

HEMT: High Electron Mobility Transistor
NCD: Nanocrystalline Diamond
PECVD: Plasma Enhanced Chemical Vapor Deposition
RIE: Reactive Ion Etch